Bulletin of Earth Sciences of Thailand

Characterization of Growth Anticline in Moattama Basin, Gulf of Moattama, Myanmar

Wongsakorn Choowala[1*], Sarawute Chantraprasert[2] and Sukonmeth Jitmahantakul[1]

[1]Petroleum Geoscience Program, Department of Geology, Faculty of Science, Chulalongkorn University,Bangkok, 10330, Thailand
[2]PTTEP, Enco, 555/1 Vibhavadi Rangsit Road, Chatuchak, Bangkok 10900, Thailand
*Corresponding author e-mail: WongsakornC@pttep.com

Abstract

Moattama Basin is underlain by the southern branch of Sagaing Fault, a major active strike-slip fault of Myanmar. According to 3D and 2D seismic reflection data, the basin has undergone faulting by the interaction between dextral deformation and gravity-driven deformation in the Gulf of Moattama. In the basin center, synchronous normal faults and a series of anticlines along an N-S dextral shear zone are observed, which may have formed by deformation above the deep-seated strike-slip fault. These anticlines form high-potential prospects for hydrocarbons. To assess this potential, structural analysis using 3D seismic data and well data was carried out to determine the geometry and evolution of the anticlines. Three anticlines were interpreted and analyzed in this study. The results show positive flower structure of all anticlines that are related to dextral shear zone and gravity-driven deformation from the Sagaing Fault. This anticline structure is very good trapped for hydrocarbon and flower structure movement can provide migration pathways for hydrocarbon.

Keywords: Positive Flower Structures, Anticline, Moattama Basin

1. Introduction

Moattama Basin covers an area of approximately > 60,000 square kilometers with sediment thickness of more than 7 km in the basin center (Morley and Alvey 2015). It is one of the most successful petroleum basins in Myanmar. Most of the structure traps within this basin are controlled by the Sagaing Fault, which is a major active right-lateral strike-slip fault (Fig. 1) (Curray 2005; Rangin et al., 2013; Morley and Alvey 2015; Racey and Ridd 2015; Rangin 2018).

Block M9 is located in the Gulf of Moattama, offshore Myanmar. The block is characterized by ENE-WSW normal faults that is resulted from dextral deformation brought on by the Indian Plate moving into Sundaland in the north direction (Soe and Watkinson, 2017). A N-S dextral shear zone in the central part of the block comprises NNW-SSE trending anticlines that appear to have developed with normal faults. The lower part of the profile of anticlines was affected in the Late Miocene-Pliocene. The activity of some anticlines continued into the Pleistocene age and was indicated by the folding of the Late Pleistocene horizons. Positive flower structures and steeply dipping faults can be interpreted beneath the anticlines. The result of transpression above a strike-slip fault zone shows the folding pattern zone in the central part of M9 (PTTEP, 2022).

This study focuses on a series of anticlines along a N-S dextral shear zone in the central part of Block M9, Moattama Basin, offshore Myanmar, which have been interpreted as a result of transpressional deformation above a deep-seated strike-slip fault zone (PTTEP, 2022). However, limited seismic data coverage prevents imaging of the fault zone, which could provide migration pathways for hydrocarbons from deep source rocks.

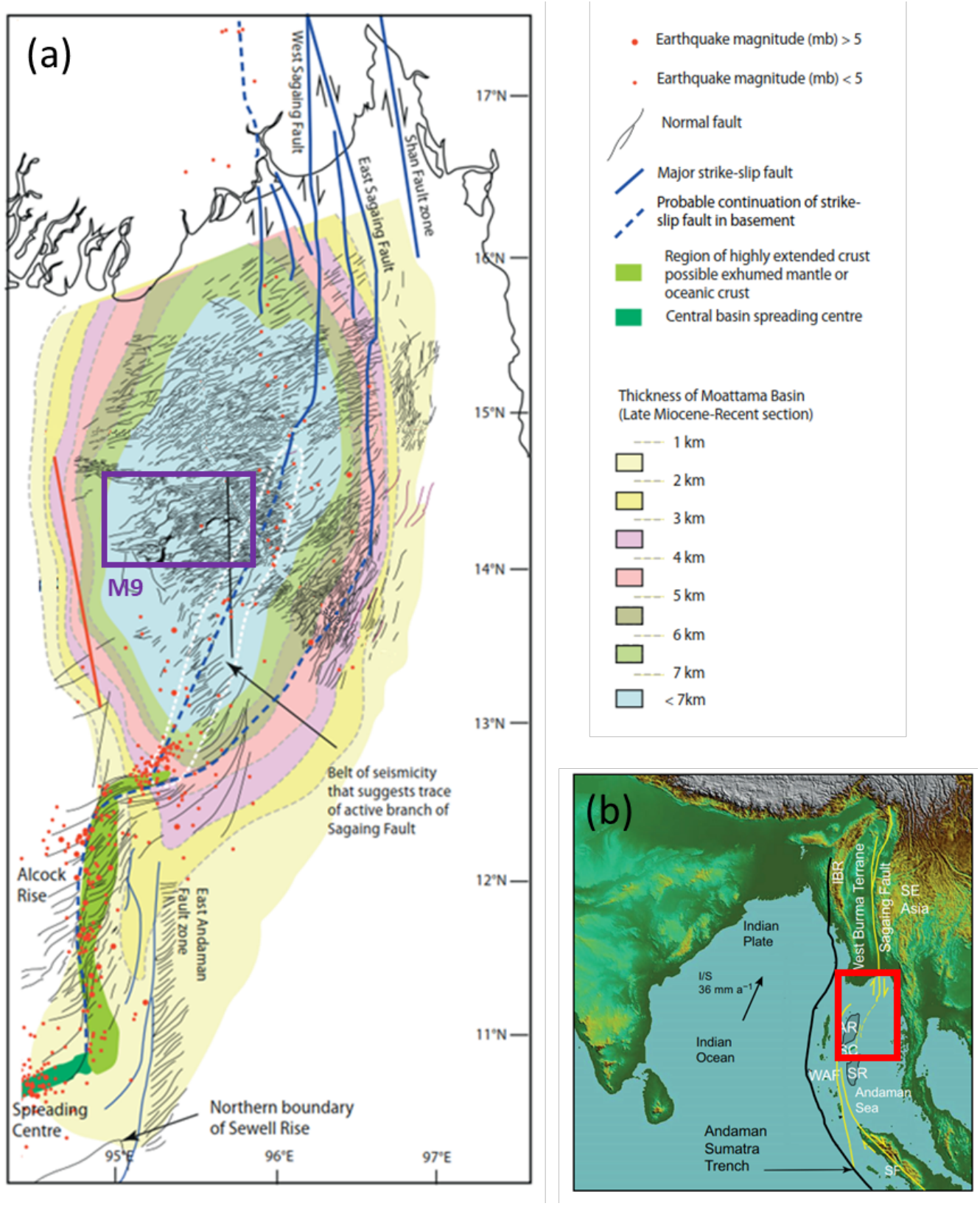

Figure 1 (a) Sedimentary thickness map and structural map of the Mottama Basin. (b) Locations of the Offshore Myanmar (Red polygon; modified after Morley, 2022).

2. Geological Settings

2.1 Regional geology

Moattama Basin is located between the Indian Plate and SE Asia (Fig. 1; Curray 2005; Rangin et al., 2013; Rangin, 2017). The basin formation followed the collision between India and Sundaland in the Late Cretaceous (Lee et al., 2006; Racey and Ridd, 2015) The Moattama Basin exhibits two major structural development stages:

1) Eocene–Early Miocene rifting: An E-W extension during Eocene to Oligocene created a N-S trough from the East Andaman Basin to the eastern Moattama region. In Early Miocene, a NNW-SSE extension generated ENE-WSW normal faults spreading across the Andaman region (PTTEP, 2022).

2) Late Miocene–Recent post-rift deformation: In the eastern part of the region, extensional and strike-slip faulting coexist with fast subsidence and a high rate of sediment deposited in Moattama from the Salween and Ayerwaddy rivers. (Morley & Alvey 2015; Racey & Ridd 2015; Liu et al. 2020). This sediment is a good reservoir and source rock for biogenic gas in Block M9 (Fig. 2).

Block M9 is dominated by ENE-WSW normal faults created by the dextral deformation due to the northward motion of the Indian Plate relative to Sundaland (Fig. 2). The central part of the Block M9 show NNW-SSE trending anticlines that appear to have developed with normal faults. The folding pattern can be interpreted as a result of transpression above a strike-slip fault zone (PTTEP, 2022).

The bending of the upper Pliocene to Resent strata indicates that certain anticlines' activity persisted into the Pleistocene. Positive flower structure and steeply dipping faults may be deduced underneath the anticlines. Due to data limitations, the structures' lowest portion and link to strike-slip fault zones are absent.

2.2 Depositional environment

This study is focused on Ayeyarwady Formation (Pliocene – Recent). This formation consists of thick marine shale interfingering with thick deltaic sandstone beds and canyon cuts in the slope area (PTTEP, 2022).

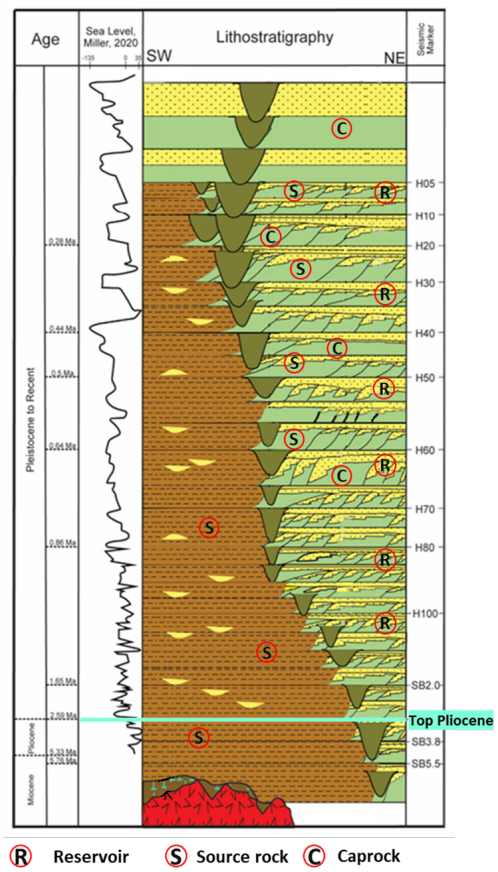

Figure 2 General stratigraphy and Petroleum system of the Moattama Basin (modified from PTTEP, 2022).

Based on biostratigraphic data, the dominant depositional environment of the Ayeyarwady Formation is deltaic shallow marine with very fine to medium-grained sandstones, with angular grains and poorly sorted, unconsolidated, and poor compaction of young sediments.

In the Plio-Pleistocene, the Moattama Basin subsided rapidly at a high rate of more than 0.75mm/my. Sediments were brought to the basin by the Salween and Ayerwaddy rivers

(Morley & Alvey, 2015; Racey & Ridd 2015; Lynn, 2019; Liu et al., 2020).

2.3 Moattama Basin petroleum system

Most of the petroleum products in the Moatama Basin are natural gas from three gas fields (Yadana, Yetagun, and Zawtika fields). The Yadana and Yetagun fields provide wet gas, while dry gas has produced from the Zawtika field as a result of biogenic generation process.

Biogenic gas is primary production in the Block M9 (Fig. 2). The biogenic generation process occurs where microorganisms decompose organic materials without oxygen and release methane at low temperatures. In addition, thermogenic gas is proved in this region, which was generated from marine shale in the Pliocene (PTTEP, 2022).

The Plio-Pleistocene marine mudstone in the Ayeyarwady Formation contains fair to good total organic carbon (TOC) concentrations (0.5-1%), with HI ranging from 100 to ~300. It is deposited in anoxic conditions immediate environment (Lynn, 2019). After biogenic gas generation, methane gas migrates along the carrier bed or fault plane to the reservoir. Deltaic and shallow marine sandstones are the main reservoirs in Moattama Basin.

The trap in the Zawtika field is a structural trap associated with normal faults. The structural domain creates by the Sagaing Fault. An intra-formational marine shale of the Plio-Pleistocene Ayeyarwady Formation acts like a seal.

2.4 Characteristics of flower structure

Flower structures are commonly used to identify strike-slip faults. Flower structures can be classified into three types, so-called negative, positive, and hybrid flower structures (Fig. 3; Huang & Liu, 2017). In the study area, anticlinal traps can be related to either positive (Fig. 3b) or hybrid flower structures (Fig. 3c). Shallow antiform and reverse faults form positive flower, which is created by upward diverging strands of a wrench fault with mostly separations (Harding, 1985). In comparison, hybrid flower structure is characterized by antiform and normal faults (Huang & Liu, 2017).

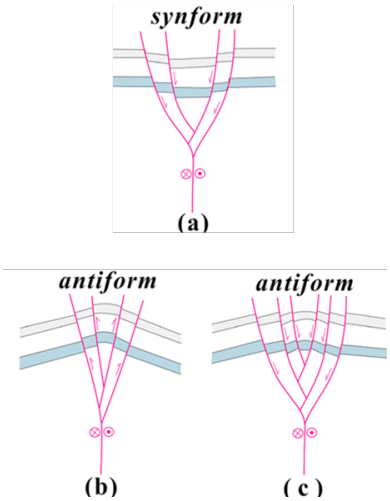

Figure 3 Types of flower structure. (a) Negative, (b) positive, and (c) hybrid flower structures (Huang & Liu, 2017).

3. Datasets and methodology

3D seismic dataset used in this study consists of two seismic cubes (Merge 2016 and M9E 2020; Fig. 4). These data cover approximately 5,015 km^2 which align in a NW-SE and E-W direction. Seismic interpretation was performed using Petrel 2021. Structural analysis involved two steps of working process. The first step included correlation of seismic and well (Well-A) to identify the Top Pliocene horizon and other sequences (H05 to H30) in the Ayeyarwady Formation. Next, these horizons were used to created time-structure maps and performed structural restoration. Anticline geometry and evolution of positive flower structure were summarized based on 3D maps and onlapping feature of growth strata above the anticlines.

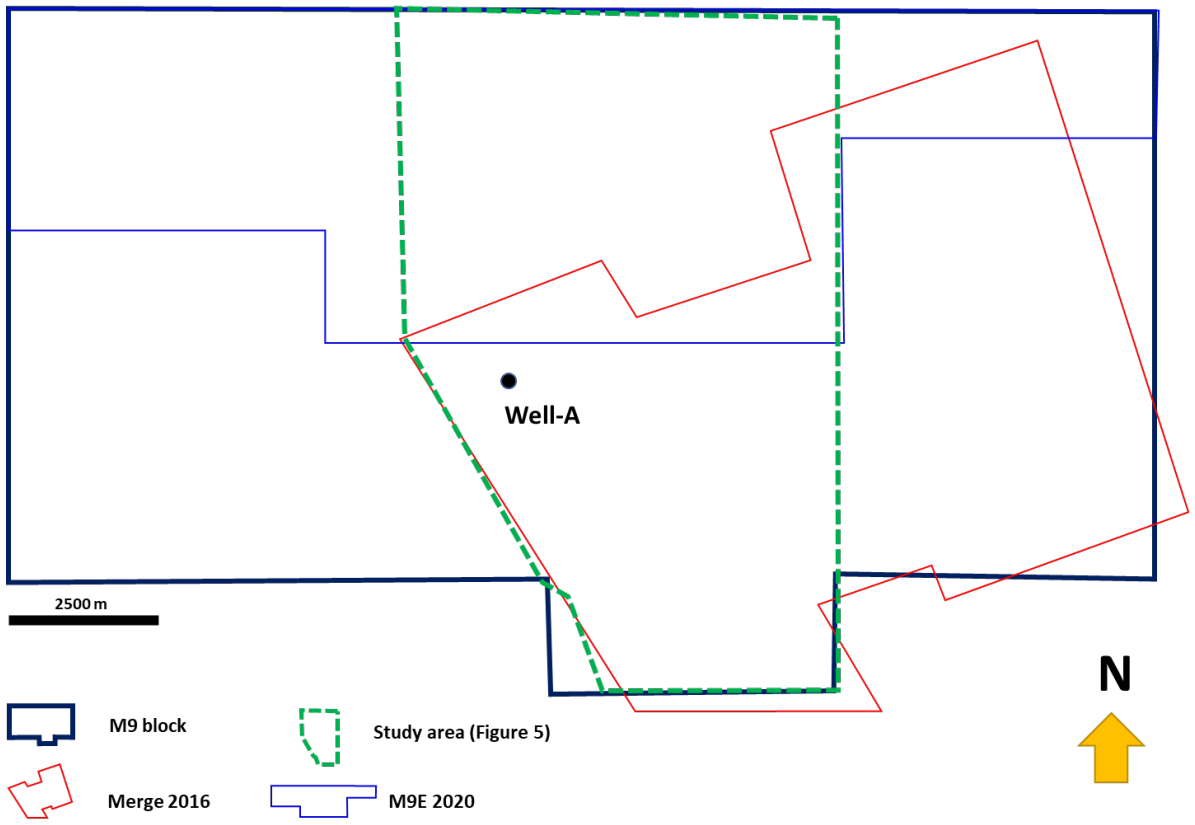

Figure 4 The well location, seismic vintages, and area of study.

4. Results

4.1 Seismic interpretation

Figure 5 shows time structure map of the Top Pliocene horizon with depth values ranging from 1 to 4 second TWT. Generally, the depth of this horizon decreases toward the SSE in association with a series of NE-SW-striking, SE-NW dipping normal faults. The map also shows the normal fault associated with NNW-SSE trending anticlines along a N-S zone about 10 km wide in the center of Block M9. Under the anticlines, positive flower structures and steeply dipping faults can be interpreted. (Figs. 6 - 8).

There are three anticlines interpreted from the seismic data (Fig.5). Their geometries are described as follows:

Anticline A

Anticline A is located in the north of Block M9. This elongate anticline has a NNW-SSE 4-way dip-closure and it is bounded in the north and south by ENE-WSW normal faults (Fig. 5). A positive flower structure with a sub-vertical center fault was interpreted at 4-6 second TWT beneath the anticline (Fig. 6). The east-dipping limb is steeper than the west-dipping limb forming an asymmetrical anticline.

Anticline B

Anticline B is about 20 km south of Anticline A. This elongate anticline has a N-S trending 3-way dip-closure and it is bounded in the south by a south-dipping normal fault (Fig. 5). A positive flower structure was interpreted at 4-5 second TWT beneath Anticline B (Fig. 7). Similar to Anticline A, the east-dipping limb is steeper than the west-dipping limb forming an asymmetrical anticline. (Fig. 7).

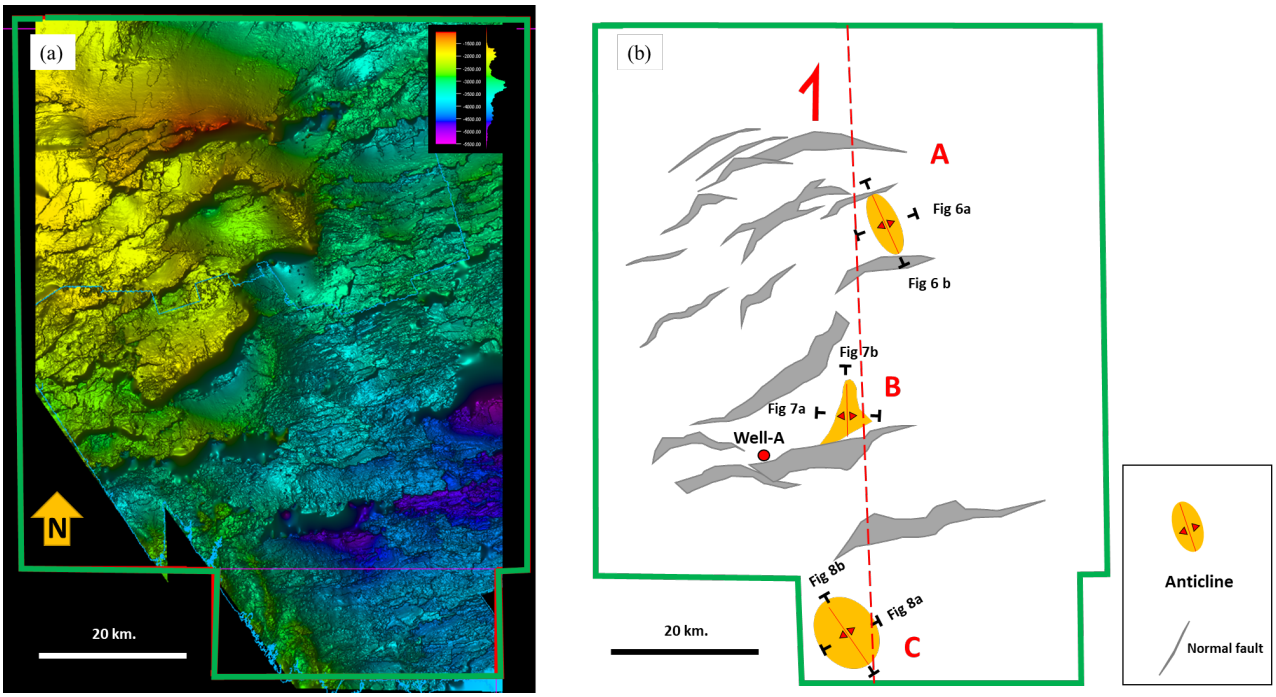

Figure 5 (a) Top Pliocene time structure map and (b) simplify model shows normal fault and anticlines N-S dextral shear zone. See Figure 4 for location.

Anticline C

Anticline C is about 30 km south of Anticline B. Due to data limitation, the closure of the structure cannot be completely delineated within the study area, and this elongate anticline has an estimated to be a NNW-SSE trending ellipse (Fig. 5). Part of positive flower structure was interpreted at 4-5 seconds TWT beneath Anticline C (Fig. 8). The east-dipping limb is also steeper than the west-dipping limb forming an asymmetrical anticline. (Fig. 8).

4.2 Timing of Folding

Simple structural restoration was performed using horizon flattening. The result showed that all anticlines developed after the deposition of the Top Pliocene horizon. Seismic reflections above the Top Pliocene onlap onto it and the seismic units above it thin over the crest of the anticlines (Figs. 9 & 10).

The configuration of seismic reflections below the Top Pliocene does not allow for the determination of deformation timing. However, we speculate that early folding episodes are likely. Folding probably continued to the deposition of sediment slightly above H05. Above the interval, the sedimentary thickness is not affected by folding and uniformed across the anticlines. Normal faults cut across the upper part of the structure between H30 and H05.

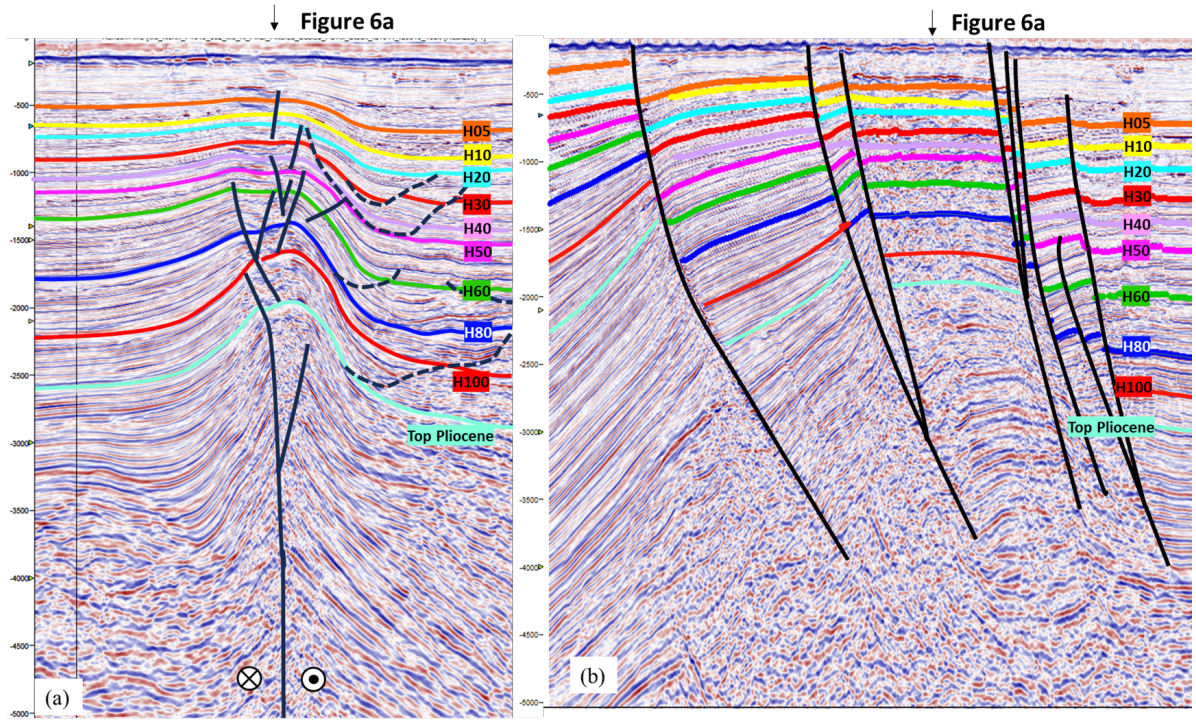

Figure 6 (a) Crossline ENE-WSW direction across anticlines A shows positive flower structure and (b) strike line NW-SE direction across anticlines A show normal fault dipping south. Line locations are shown in Figure 5.

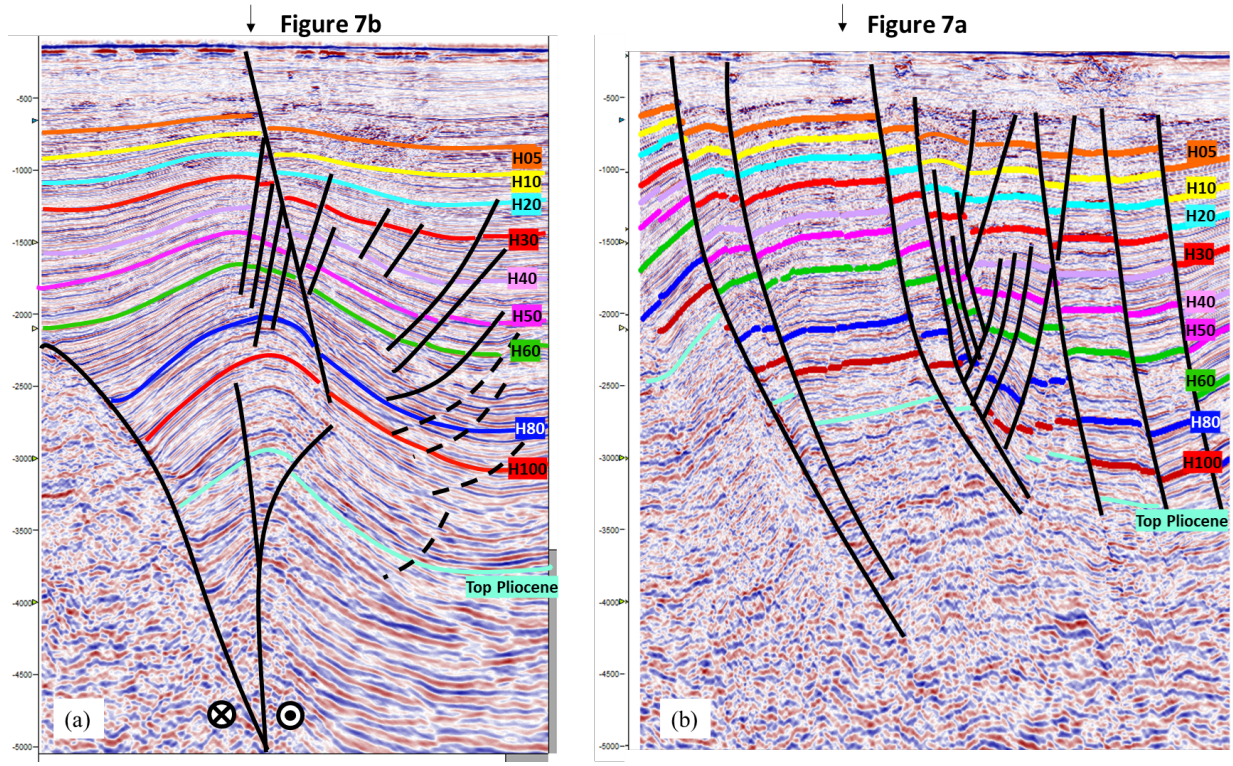

Figure 7 (a) Crossline ENE-WSW direction across anticlines B shows positive flower structure and (b) strike line NW-SE direction across anticlines B show normal fault dipping south. Line locations are shown in Figure 5.

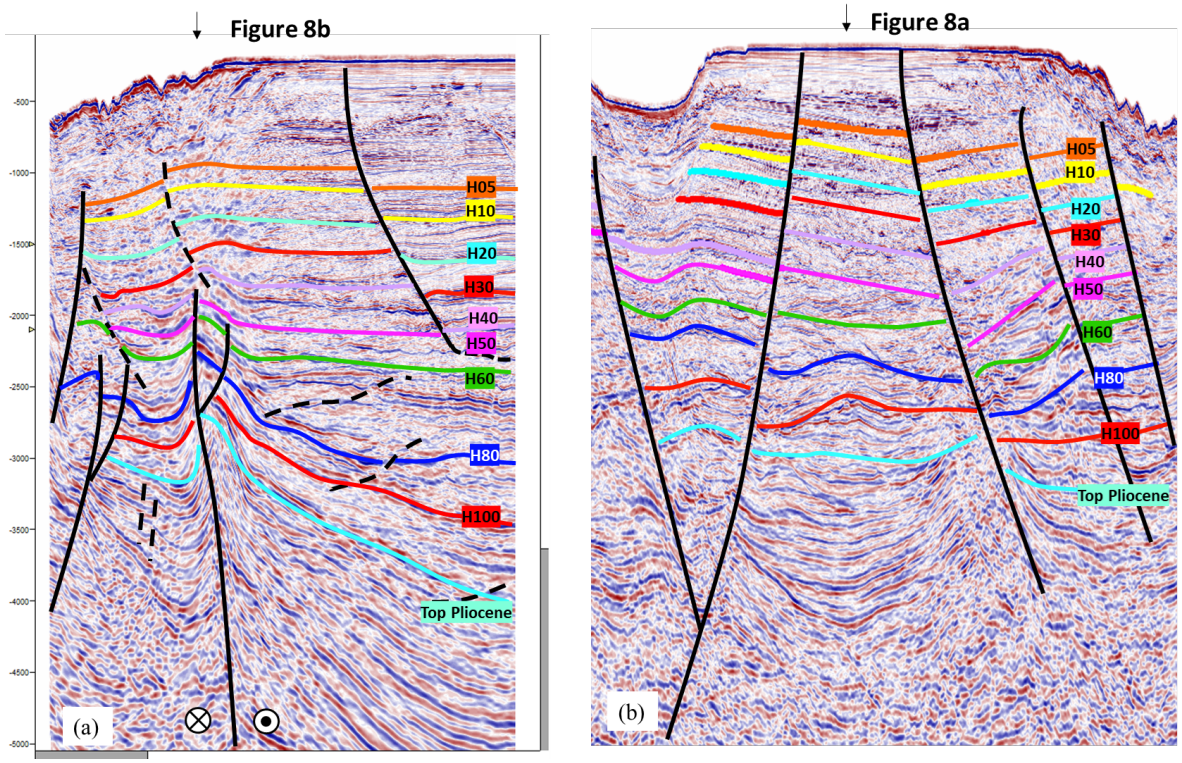

Figure 8 (a) Crossline ENE-WSW direction across anticlines C shows positive flower structure and (b) strike line NW-SE direction across anticlines C show normal fault dipping south. Line locations are shown in Figure 5.

5. Discussion

5.1 Origin of Anticlines

Structural analysis in the study area focuses on the geometries and orientation of the anticlines within a dextral shear zone. The anticlines are oriented NNW-SSE (Anticline A&C) and N-S (Anticline B). We interpret that the anticlines of both orientations developed together during the Miocene-Pleistocene transpression (PTTEP, 2022).

The geometric characteristics of the anticlines and positive flower structures are similar to the strike-slip analogue models for the Bohai Bay Basin (Fig. 3) by Huang & Liu (2017). The positive flower structures in the Bohai Bay Basin comprises anticlines and steeply dipping convex-upward reverse faults.

Normal faults are interpreted within the upper part of the some of the anticlines (Figs. 9 & 10). These normal faults could have resulted from flexural stretching across the crest of the anticlines (Fig. 10). However, other normal faults may have developed during later gravity-influenced transtension, which created most of the faults in the eastern part of M9 (Morley et al. 2022).

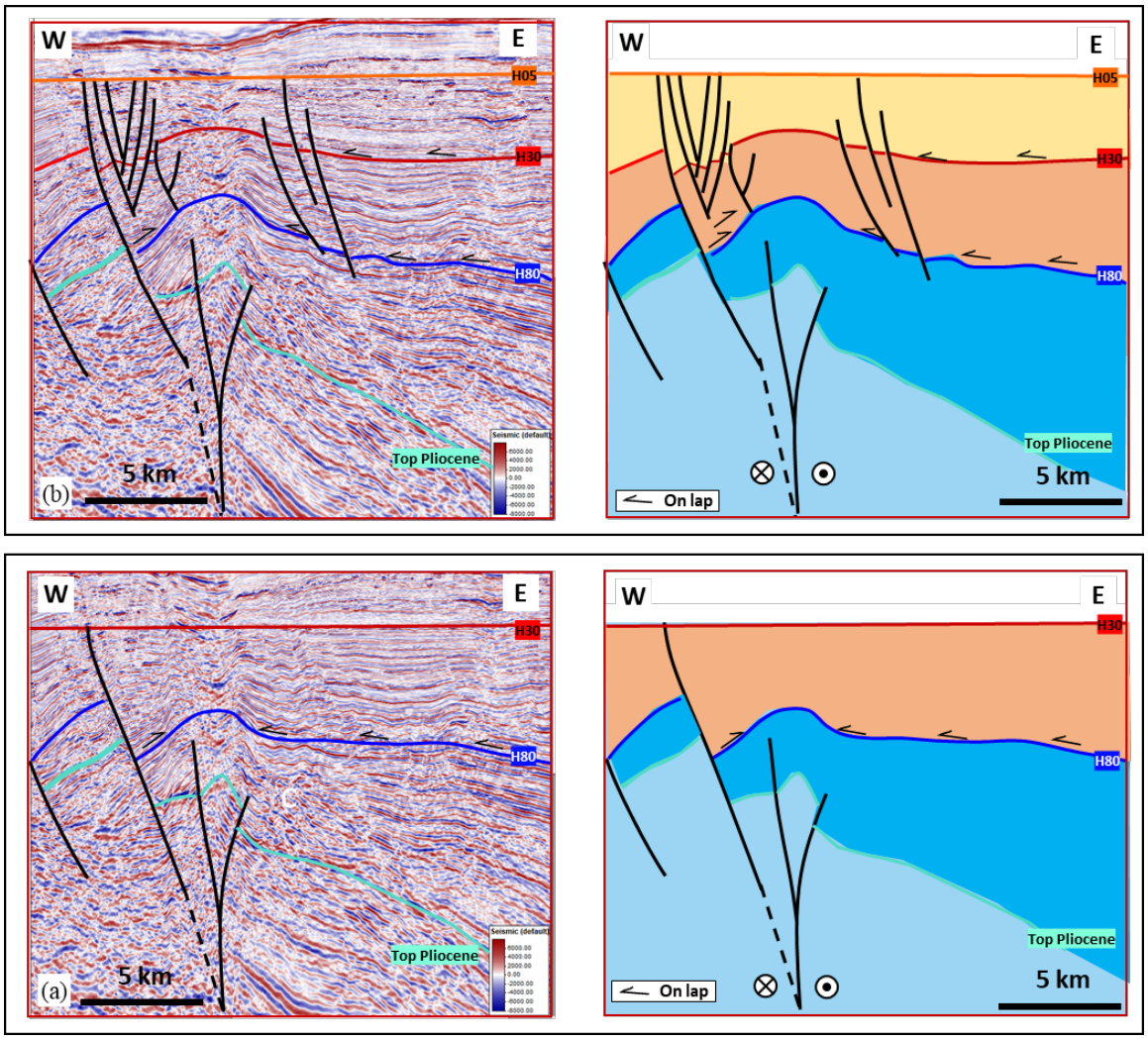

Figure 9 Restoration of the Anticline A, left shows seismic restoration, and right shows line drawing from seismic lines; (a) H30, and (b) H05 (See Fig. 5a for location).

5.2 Analogue models vs seismic interpretation.

Preliminary attempts have been made to model the effects of transpression within a sedimentary section above a deep strike-slip zone using a sandbox modelling technique. Experiments were conducted using 7-cm-thick sand layers to mimic the 7-km-thick sediments in the Mottama Basin. This scaling ratio of 10^{-5} between the model and natural prototype is commonly used in analogue model labs (PTTEP, 2022). Representative result is shown in Figure 11. Dextral transpression deformation was performed by moving one side of the model dextrally towards the other side, which is fixed.

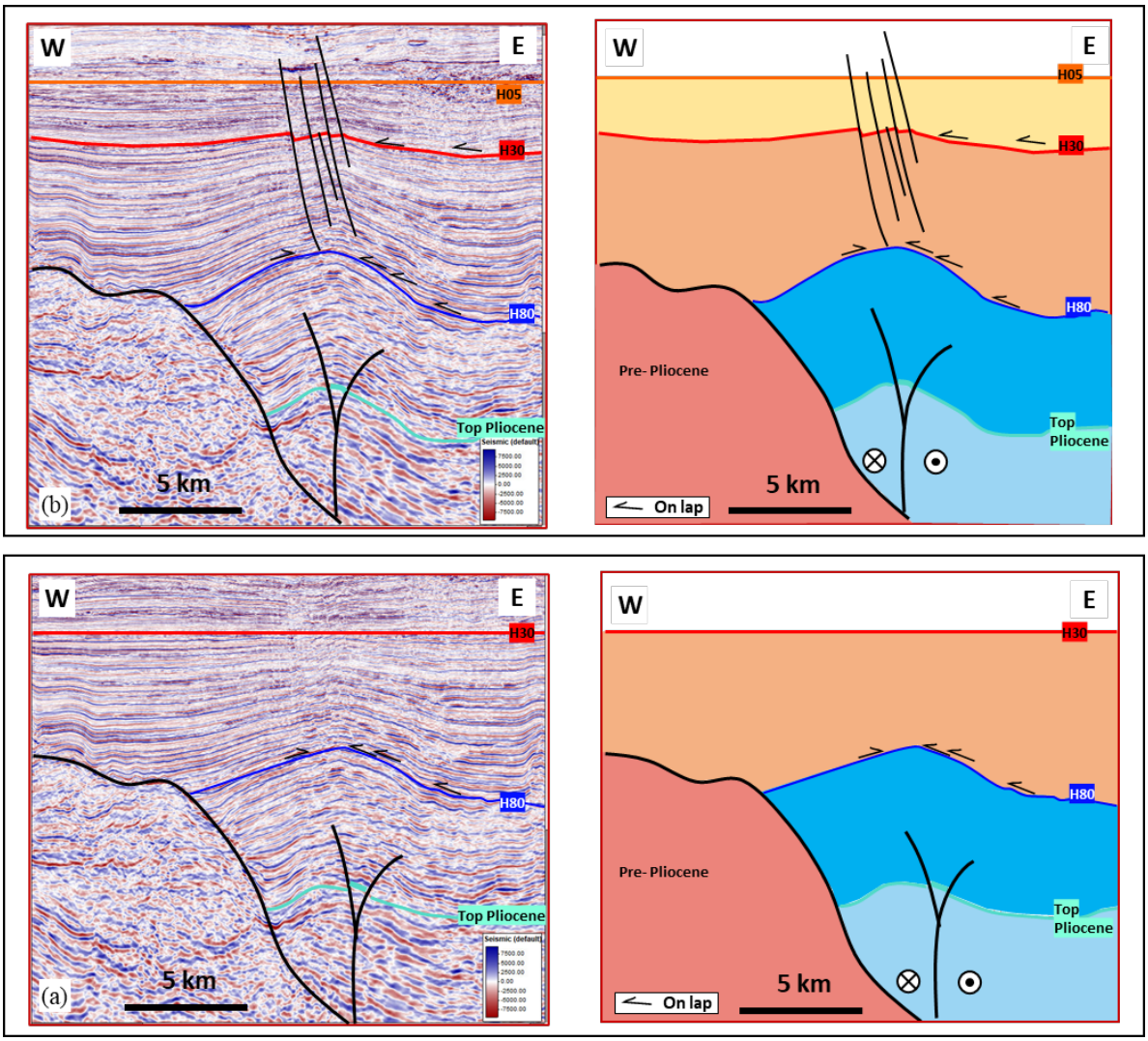

Figure 10 Restoration of the Anticline B, left shows seismic restoration, and right shows line drawing from seismic lines; (a) H30, and (b) H05 (See Fig. 5a for location).

After 4 cm of strike-slip movement and 1.6 cm compression, a large anticline formed parallel to the underlying shear zone between a pair of convergent-dipping reverse faults. In cross-section, growth strata (the red sand layer in Fig. 11) thicken away from the fold axis. This feature can also be found in anticlines A and B (Figs 6 & 7). However, considering the scaling ratio above, the anticlines interpreted in the study area should be comparable to the small, millimeters-high, en echelon anticlines that developed during the early part of the experiments, after 1-2 cm strike-slip displacement. These would correspond to the anticlines with 100s m of vertical relief observed in the seismic data. The small relief of the sandbox model anticlines prevents their proper imaging. Alternative and better appropriate technology is required to document the geometries such low-relief structures in sandbox models.

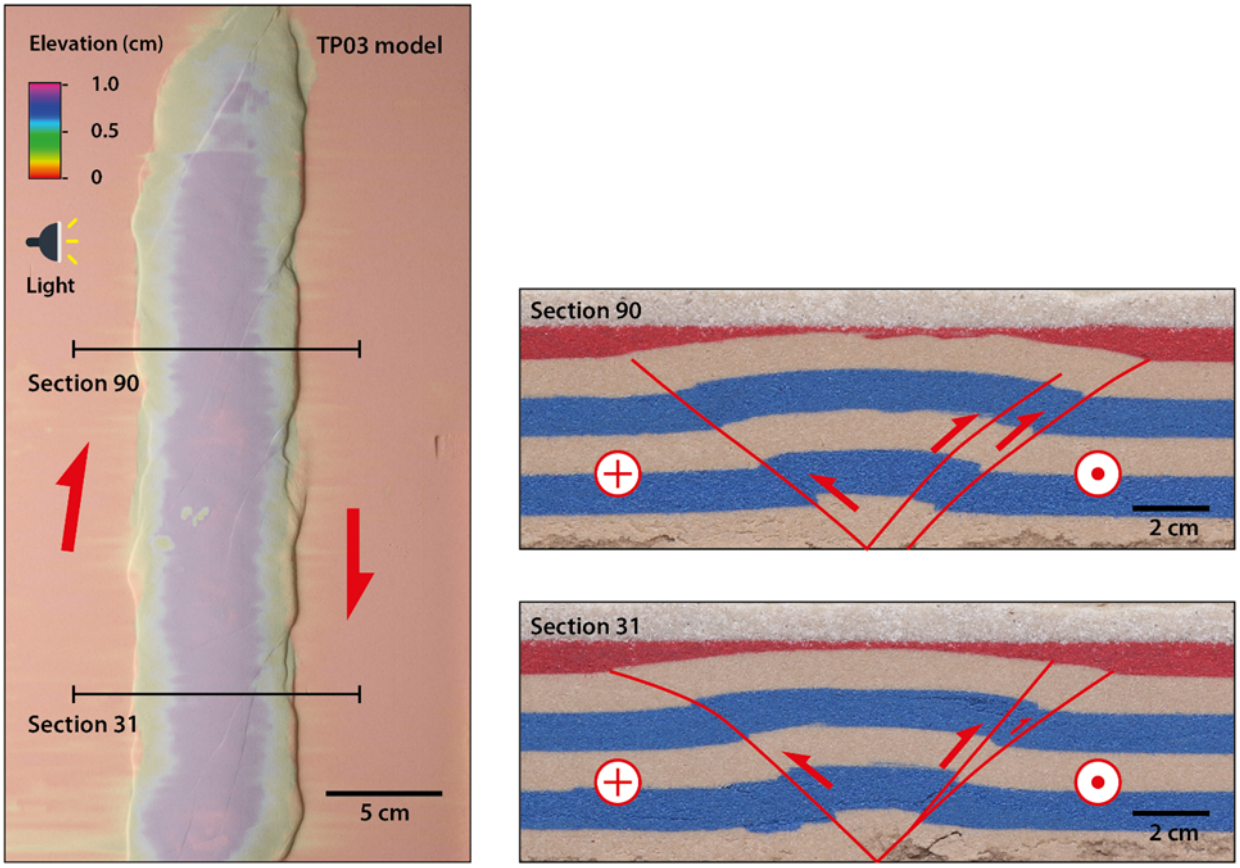

Figure 11 Top-view photograph of Model TP03 after 4cm displacement of dextral strike-slip fault with 1.6cm shortening. Elevation of top model surface highlights elongate symmetrical anticline formed by convergent-down dipping reverse faults (left). Model sections with fault interpretation showing anticline above the basement strike-slip fault. This model does not produce internal deformation within the anticline (right).

5.3 Implications for Hydrocarbon Exploration

Previous drilling has proven that transpression anticlines provide effective petroleum traps, particularly where they involve the deltaic sand-shale sequence such as those in the study area. Similar structures have been proven prospective in other strike-slip terrains, such as the Los Angeles Basin, along the San Andreas Fault (Wright, 1991) and the Myanmar Central Plains (Racey & Ridd 2015). While most gas accumulations in east of the study area have biogenic origins, the anticlines in the study area have additional potential of thermogenic gas, as the strike-slip and reverse faults associated with them appear to continue to deeper levels and provide migration conduits from thermogenic kitchens.

Hence, the antiform structures A, B, and C in this study, as well as similar structures along comparable trends in the Moattama Basin could be a new exploration target.

6. Conclusion

This study incorporates a seismic interpretation of 3D seismic data from Block M9, Moattama basin, Myanmar to understand the anticline in the central of Block M9. Three anticline structures are interpreted to have developed above strike-slip flower structures with steeply dipping strike-slip and reverse faults. The structures likely developed during

the Late Miocene to Pleistocene dextral transpression of an existing N-S trending structure that could be a branch of the Sagaing Fault or other geological discontinuity.

The anticline structures were generated in sandbox experiments as low-relief en echelon structures after a few centimeters of dextral strike-slip motions, equivalent to a few kilometers of slip in nature.

The anticlines have been proven effective petroleum traps with potential for both biogenic and thermogenic gas. Similar structures within the same trend or comparable trends in the Gulf of Moattama should provide new exploration target that require further detailed study and evaluation.

Acknowledgments

We would like to give thanks to PTT Exploration and production Public Company Limited. (PTTEP) and Myanmar Oil and Gas Enterprise (MOGE) for supporting the permission to use M9 data. Sorasak Lendam, Athittan Prueksuwat, and GST teams from PTTEP are thanks for giving guidance and suggestions. The first author would like to thank PTTEP for full scholarship of M.Sc. Petroleum Geoscience program at Chulalongkorn University.

References

Allen, P. A., & Allen, J. R. 2013. *Basin analysis: Principles and application to petroleum play assessment.* John Wiley & Son, Oxford. pp 640.

Curray, J.R. 2005. Tectonics and history of the Andaman Sea. *Journal of Asian Earth Sciences,* 25, 187-232.

Harding, T. P. 1985. Seismic characteristics and identification of negative flower structures, positive flower structures, and positive structural inversion. *AAPG Bulletin,* 69, 585-600.

Huang, L., & Liu, C.-Y. 2017. Three types of flower structures in a divergent-wrench fault zone. *Journal of Geophysical Research: Solid Earth,* 122, 10,478-10,497.

PTTEP, 2022, Gulf of Moattama Regional Petroleum Geology. Unpublished report. PTTEP, Bangkok, Thailand.

Lee G. H., Kim B., Shin K. S. & Sunwoo D. 2006. Geologic evolution and aspects of the petroleum geology of the northern East China Sea shelf basin. *AAPG bulletin,* 90, 237-260.

Liu, J.P., Kuehl, S.A., Pierce, A.C., Williams, J., Blair, N.E., Harris, C., Aung, D.W. & Aye, Y.Y. 2020. Fate of Ayeyarwady and Thanlwin River Sediments in the Andaman Sea and Bay of Bengal. *Marine Geology,* 423, 106137,

Lynn M., 2019. Biogenic Gas Potential of Myanmar. Proceedings on *The 4th AAPG/EAGE/MGS Myanmar Oil and Gas Conference,* 13-15 November 2018. Myanmar.

Morley, C.K. Chantraprasert, S., Chenoll, K., Sootlek, P. & Jitmahantakul, S. 2022. Interaction of thin-skinned detached faults and basement-involved strike-slip faults on a transform margin: the Moattama Basin, Myanmar. *Geological Society, London, Special Publications,* 524, 165-190.

Morley, C.K. & Alvey, A. 2015. Is spreading prolonged,episodic or incipient in the Andaman Sea? Evidence from deepwater sedimentation. *Journal of Asian Earth Sciences,* 98, 446-456.

Rangin, C. 2017. Chapter 3. Active and recent tectonics of the Burma Platelet in Myanmar. *Geological Society, London, Memoirs,* 48, 53-64.

Rangin, C., Maurin, T. & Masson, F. 2013. Combined effects of Eurasia/Sunda

oblique convergence and East-Tibetan crustal flow on the active tectonics of Burma. *Journal of Asian Earth Sciences,* 76, 185-194.

Rangin, C. 2018. *The Western Sunda basins and the India/Asia Collsion: An Atlas*. Geotecto, Paris, France. pp 249.

Racey, A. & Ridd, M.F. 2015. Petroleum geology of the Moattama region, Myanmar. *Geological Society, London, Memoirs,* 45, 63-81.

Soe, T.T. & Watkinson, I.M. 2017. Chapter 19: the Sagaing Fault. *Geological Society, London, Memoirs,* 48, 413-441.

Wright, T. L. 1991. Structural geology and tectonic evolution of the Los Angeles basin, California. *Active margin basins*, Tulsa, Oklahoma, the United States.